XIX IMEKO World Congress
Fundamental and Applied Metrology
September 6−11, 2009, Lisbon, Portugal

MULTI-STEREO COMPATIBILITY ANALYSIS FOR 3D SHAPE ESTIMATION

M. De Cecco [1], M. Pertile [2], L. Baglivo [1], G. Parzianello [1], M. Lunardelli [1], F. Setti [1] , A. Selmo [3]

[1] Department of Mechanical and Structural Engineering, University of Trento, Via Mesiano 77, 38100 Trento (TN), Italy
[2] Dept of Mechanical Engineering, University of Padova, Via Venezia 1, 35131 Padova (PD), Italy
[3] Dept of Information Engineering, University of Padova, Via Gradenigo 6/B, 35131 Padova (PD), Italy

Abstract − A method for the reconstruction of a 3D shape is described and applied to a practical measurement case. Multiple stereo systems are employed to measure a 3D surface with superimposed colored markers. The described procedure comprises a detailed uncertainty analysis of all the measurement phases, and a statistical compatibility analysis of the colored markers measured by different stereo pairs. The compatible acquired markers are statistically merged in order to obtain a measurement of a 3D shape and an evaluation of the associated uncertainty. The obtained results show that the selected experimental set-up allows to considerably reduce the uncertainty associated to the fused points. The selection of a limit distance, that divides compatible points from not compatible ones, is also presented.

Keywords: multiple stereo systems; uncertainty evaluation; 3D shape reconstruction.

1. INTRODUCTION

3D shape reconstruction using vision systems is a technique widely used to reconstruct spatial objects and a lot of algorithms and methods are available in literature. The use of multiple pairs of cameras allows the reconstruction of different portions visible by each pair, and then their fusion to obtain the complete shape. In this way each pair can be optimized for its interest region, increasing thus the accuracy of each partial reconstruction. Several methods can be used to match the information on different cameras: shape detection, edge detection, correlation analysis of different portions of the image, marker matching in the two views or others. For instance, [1] describes a method for surface reconstruction that employs a Lagrangian polynomial for surface initialization and a quadratic variations method to improve the results. [2] recovers a first approximation of the shape through the object silhouettes seen by the multiple cameras and then improves the shape through a carving approach, employing local correlation analyses between images taken by different cameras. This approach relies on the hypothesis that, if a 3D point belongs to the object surface, its projection into the different cameras which really see it will be closely correlated. In [3] a method for spatial grouping of 3D points viewed by multiple stereo systems is presented. The grouping algorithm comprises a 3D space compressing step in order to map the 3D points into a space of even density that allows an easier grouping through a neighborhood approach; a subsequent uncompressing step preserves the adjacencies of the compressed space and helps the fusion of grouped points seen by different cameras.

One of the most important aspects of the reconstruction is the fusion of data coming from different stereo pairs, as some portions of the object may not be visible from one or more pairs. The process of merging images requires the use of techniques to decide whether points should be merged or not. One promising method is associating uncertainty to each reconstructed point of each pair and making decisions relying also on this information.

A drawback of the approaches cited above is that they do not evaluate the uncertainty of the reconstructed object. If a multiple stereo system is used to perform measurements, it is highly recommended to evaluate a region of confidence of the measured 3D points or objects, with a desired level of confidence. The method described in this work employs a detail uncertainty analysis with two goals: merging the measurement performed with different stereo pairs and at the same time obtaining the uncertainty associated with the measured quantities.

Each step of the measurement process is affected by uncertainty that propagates to the final 3D reconstructed model and may de-qualify the results obtained. Uncertainty derives from a multitude of causes, such as noise in the image acquisition, defocusing, evaluation of the intrinsic and extrinsic parameters of the cameras, depth estimation of the physical point, choice of the points to merge and merging method for the final fusion of 3D parts.

In [4] an uncertainty analysis is presented for a binocular stereo reconstruction, but a method to compare and fuse the measurements of different stereo pairs is not described. A method to fuse the measurements of different stereo pairs is described in [5]. In this case, however, the uncertainties associated with the intrinsic and extrinsic camera calibration parameters are neglected, and a simplified geometrical uncertainty propagation algorithm is employed. In the present work, particularly for multiple stereo fusion, a detailed uncertainty analysis is performed using the general method described in the GUM [6] and its supplement 1 [7]. Furthermore, the described procedure includes a statistical compatibility analysis, performed before the fusion of different stereo pairs.

The reconstruction presented is based on the acquisition of colored markers superimposed on the shape to be reconstructed by means of pairs of cameras; the centroid of each marker is detected on each camera and matching position of markers is performed using both epipolar geometry and color matching to improve robustness of matching. Depth evaluation is done for each pair, and the compatibility of the points measured by different stereo pairs is analyzed; eventually, the fusion of compatible points is performed on a common reference frame for all cameras.

The steps of uncertainty evaluation described in the following allow to associate a covariance matrix with each 3D point reconstructed by each stereo pair. The information contained in the uncertainty ellipsoid is the basis for verifying the compatibility of 3D points acquired by different stereo pairs, for merging compatible points and estimating their uncertainty. Using such a process, each point reconstructed in the 3D space is not only identified by its coordinates, but also is associated with an uncertainty ellipsoid deriving from the whole reconstruction process. This information is necessary for points interpolation using surfaces to minimize a cost function that takes into account not only point positions, but also point uncertainties, improving significantly final results.

In the following sections, the employed method is first described (sections 2-5) with a detailed uncertainty analysis and then it is applied to the measurement of a 3D shape with superimposed colored markers; some laboratory results are presented in section 6.

2. STEREO CAMERA MODEL

As described in [8], a stereo system comprises two cameras 1 and 2 and each camera has a corresponding frame of reference having the z axis aligned with the optical axis (a figure will be added in the final version of the work). Taking into consideration the model of each camera, it is possible to write the generic position of a point feature comprised in the field of view of both cameras:

$$ {}^{i}\mathbf{X} = {}^{i}\begin{bmatrix} X \\ Y \\ Z \end{bmatrix} = \lambda_i \begin{bmatrix} x_i \\ y_i \\ 1 \end{bmatrix} = \lambda_i \mathbf{x}_i \qquad (1) $$

where i can be 1 or 2, depending on which camera is taken into account; ${}^{1}\mathbf{X}$ (or ${}^{2}\mathbf{X}$) is the point position expressed in the frame 1 (or 2) associated with camera 1 (or 2); $\mathbf{x}_1$ (or $\mathbf{x}_2$) is the projection of the point ${}^{1}\mathbf{X}$ (or ${}^{2}\mathbf{X}$) using an ideal camera aligned as the camera 1 (or 2) and having focal length equal to 1 (in length units); $\lambda_i \in \mathbb{R}^+$ is a scalar parameter associated with the depth of the point.

Each camera is characterized by a set of intrinsic parameters that are evaluated during camera calibration, as described below in the calibration uncertainty section, and define the functional relationship between the projection $\mathbf{x}_i$, expressed in length units, and the projection $\mathbf{x}'_i$, expressed in pixels (x'_i and y'_i are respectively the number of columns and the number of rows from the upper left corner of the sensor); using an ideal pinhole camera it is possible to find out the following direct model:

$$ \mathbf{x}'_i = \begin{bmatrix} x'_i \\ y'_i \\ 1 \end{bmatrix} = \begin{bmatrix} 0 & f_m \cdot s & x'_{0,i} \\ -f_m & 0 & y'_{0,i} \\ 0 & 0 & 1 \end{bmatrix} \begin{bmatrix} x_i \\ y_i \\ 1 \end{bmatrix} = \mathbf{K} \cdot \mathbf{x}_i \qquad (2) $$

where $f_m = f \cdot Sx$; $s = \dfrac{Sy}{Sx}$; $Sx = \dfrac{pixels}{length \quad unit}$ along x axis (not x'); $Sy = \dfrac{pixels}{length \quad unit}$ along y axis (not y'); f is the focal length in length units; $x'_{0,i}$, $y'_{0,i}$ are the distances (respectively in pixel columns and rows) between the upper left corner and the principal point (intersection of the optical axis with the sensor).

3. TRIANGULATION

If both cameras of the stereo system are calibrated, it is possible to measure the 3D position of a feature point in space using a triangulation algorithm. In this paper, the algorithm of the middle point is used for triangulation. In theory, when a point feature in space $\mathbf{X}$ is acquired by both cameras, the preimage lines that project the point $\mathbf{X}$ into the sensors should intersect in the point $\mathbf{X}$ itself. In practice, due to measurement uncertainty, the acquired preimage lines does not intersect each other. Thus, the employed algorithm, starting from the projected points $\mathbf{x}'_i$, finds the 3D points $\mathbf{X}_{1,s}$, $\mathbf{X}_{2,s}$ with the minimum distance and belonging respectively to the preimage lines of camera 1 and 2. Points $\mathbf{X}_{1,s}$, $\mathbf{X}_{2,s}$ define a segment orthogonal to the two skew preimage lines. The middle point $\mathbf{X}_m$ of this segment is selected as the measured 3D point of the feature.

4. UNCERTAINTY ANALYSIS

In the triangulation algorithm, the triangulated point $\mathbf{X}_m$ is computed from the values of the following quantities: 1) $\mathbf{x}'_i$ (i=1,2) which are the projections of the 3D point $\mathbf{X}$ in the cameras 1 and 2, and are supposed to be known from measurement (the evaluation of the uncertainty of $\mathbf{x}'_i$ is described the following 4.2 subsection); 2) $f_{m,i}$, s_i; $x'_{0,i}$, $y'_{0,i}$, which are the intrinsic calibration parameters of cameras; 3) ${}^{w}\mathbf{P}_{0i}$ which are the origin positions of the camera frames; 4) α_i, β_i, γ_i, which are the Euler angles defining the rotation of the camera frame i with reference to the world frame. ${}^{w}\mathbf{P}_{0i}$, α_i, β_i, γ_i are the extrinsic calibration parameters of cameras. Both intrinsic and extrinsic parameters with their uncertainties are evaluated by calibration as described in the following 4.1 subsection.

4.1 Calibration uncertainty

The parameters previously defined in the camera model are estimated through camera calibration. The procedure that is employed is similar to the one proposed by Tsai, see [9], with a planar target which translates orthogonal to itself, generating a three-dimensional grid of calibration points. At a first step the parameters are obtained using a pseudo-inverse solution of a least-squared problem employing points on the calibration volume and image points. After this first estimation of the intrinsic and extrinsic parameters, an iterative optimization is performed in order to minimize the errors between acquired image points and the projections of the 3D calibration points on the image plane using the estimated parameters.

Before using the algorithm of calibration , optical radial distortions are estimated and adjusted by rectifying the distorted images. Radial distortion coefficients are estimated by compensation of the curvature induced by radial distortion on the calibration grid [10].

The camera parameter uncertainties are evaluated propagating the uncertainties of the 3D calibration points and those of image points, see [4], [9]. The propagation is performed by a Monte Carlo simulation.

The reasons of deviation between measured image points and the projection of 3D calibration points on the image plane are various: simplification of camera model, camera resolution, dimensional accuracy of the calibration grid, geometrical and dimensional accuracy of grid translation. Considering that the motion of the grid to generate a calibration volume is not perfectly orthogonal to the optical axis of the camera, a bias is induced in the uncertainty distribution of the grid points and so the uncertainty becomes not symmetric. In order to take this into account, other two parameters are introduced to characterize the horizontal and vertical deviation from orthogonality.

4.2 Matching uncertainty

The point $\mathbf{X}$ in the 3D space is defined as a centroid of a circular marker; for this reason the determination of the projection $\mathbf{x}'_i$ on the CCD of the point $\mathbf{X}$ is always affected by uncertainty. Firstly the digitalization and successive binarization of the image deforms the circular shape in a polygonal shape and the centroid of these two shapes is not the same. Secondly the marker, that was originally a circle, is deformed in order to adhere to the surface of the target; as a first approximation, the deformed marker can be expressed by an ellipse. Thirdly, due to the perspective effects, an ellipse that is not perpendicular to the optical axis of the camera is projected on the CCD as an ovoid.

A simplified model for the perspective geometry identifies each marker projection as an ellipse; a method to fit this ellipse is the use of the covariance matrix of the distribution of the pixels recognized as marker. Then, it is possible to compare the projected marker with the corresponding covariance ellipse (estimated at a set confidence) and to compute two parameters $\Delta_{Cf\,it}$, $\sigma^2_{f\,it}$ that express the "difference" between the projected ovoid and the estimated ellipse; $\Delta_{Cf\,it}$ and $\sigma^2_{f\,it}$ are respectively the mean vector and the standard deviation of the distance between the edge points of the projected marker and the covariance ellipse at 99% of confidence.

The uncertainty of the computed ellipse centroid is considered a function of these two parameters:

$$f\left(\Delta_{Cf\,it}, \sigma^2_{f\,it}\right)$$

The larger is the difference between the projected ovoid and the estimated ellipse and the larger is the uncertainty associated with the computed centroid. This function is evaluated by a calibration procedure, which comprises the variation of the marker orientation and position of known steps using a planar marker and a marker adherent to a cylindrical lateral surface.

4.3 Uncertainty propagation

The uncertainty evaluation for the triangulated point $\mathbf{X}_m$ becomes an uncertainty propagation problem, which employs the functional model between input quantities ($\mathbf{x}'_i$, $f_{m,i}$, s_i ; $x'_{0,i}$, $y'_{0,i}$, ${}^{w}\mathbf{P}_{0i}$, α_i , β_i , γ_i) and output ones (three components of $\mathbf{X}_m$):

$$\mathbf{X}_m = f\left(\mathbf{x}'_i, f_{m,i}, s_i, x'_{0,i}, y'_{0,i}, {}^{w}\mathbf{P}_{0i}, \alpha_i, \beta_i, \gamma_i\right) \qquad (2)$$

with i=1,2.

Different uncertainty propagation methods are known. All of them are based on an information representation theory (i.e. probability or possibility or evidence theory), and uses a corresponding means for uncertainty expression (i.e. probability density functions or fuzzy variables or random-fuzzy variables). According to the GUM [6], in this work, the uncertainty is analyzed using the probability theory and is expressed by probability density functions (PDFs). In order to calculate the propagated uncertainty of the triangulated position $\mathbf{X}_m$ taking into account the contributions of all uncertainty sources that may contribute, the method based on the formula expressed in the GUM [6] is used. This method is selected, instead i.e. of the Monte Carlo propagation approach to increase the computation speed and to allow a real time implementation. The propagation formula uses the sensitivity coefficients obtained by linearization of the mathematical model; this method is based on the hypothesis that a probability distribution, assumed or experimentally determined, can be associated to every uncertainty source considered, and that a corresponding standard uncertainty can be obtained from the probability distribution.

The GUM proposes a formula for the calculation of the uncertainty to be associated with the output quantities $\mathbf{X}_m$, obtainable as an indirect measurement of all input quantities: $\mathbf{U}_{out} = \mathbf{c} \cdot \mathbf{U}_{in} \cdot \mathbf{c}^T$; where $\mathbf{U}_{in} \in \mathbb{R}^{24\times24}$ is the covariance matrix associated with the input quantities, which are 24 in this application; $\mathbf{U}_{out} \in \mathbb{R}^{3\times3}$ is the covariance matrix associated with the output quantities, which are the three components of $\mathbf{X}_m$; $\mathbf{c} \in \mathbb{R}^{3\times24}$ is the matrix of the sensitivity coefficients achievable from partial derivatives of f() with respect to input variables:

$$c_{i,j} = \frac{\partial f_i}{\partial input_j}$$

In this application, the following assumptions are made:

a) The two components of $\mathbf{x}'_i$ of each camera are assumed cross-correlated among themselves and not correlated with all other input quantities;

b) The intrinsic calibration parameters of each camera are assumed cross-correlated among themselves and not correlated with the corresponding parameters of the other camera and all other input quantities;

c) The extrinsic calibration parameters of each camera are assumed cross-correlated among themselves and not correlated with the corresponding parameters of the other camera and all other input quantities;

With these assumptions it is possible to build the 24x24 covariance matrix of input quantities putting six reduced dimension covariance matrices along the diagonal of $\mathbf{U}_{in}$ and assigning zero values to all other elements of $\mathbf{U}_{in}$:

$$\mathbf{U}_{in} = \begin{bmatrix} \mathbf{U}_{\text{meas},1} & \mathbf{0} & \cdots & \cdots & \cdots & \mathbf{0} \\ \mathbf{0} & \mathbf{U}_{\text{meas},2} & \mathbf{0} & \cdots & \cdots & \cdots \\ \cdots & \mathbf{0} & \mathbf{U}_{\text{int},1} & \mathbf{0} & \cdots & \cdots \\ \cdots & \cdots & \mathbf{0} & \mathbf{U}_{\text{int},2} & \mathbf{0} & \cdots \\ \cdots & \cdots & \cdots & \mathbf{0} & \mathbf{U}_{\text{ext},1} & \mathbf{0} \\ \mathbf{0} & \cdots & \cdots & \cdots & \mathbf{0} & \mathbf{U}_{\text{ext},2} \end{bmatrix}$$

where $\mathbf{U}_{\text{meas},1} \in \mathbb{R}^{2\times2}$ is associated with the measurement $\mathbf{x}'_1$ of camera 1; $\mathbf{U}_{\text{meas},2} \in \mathbb{R}^{2\times2}$ is associated with the measurement $\mathbf{x}'_2$ of camera 2; $\mathbf{U}_{\text{int},1} \in \mathbb{R}^{4\times4}$ is associated with the intrinsic parameters $f_{m,1}, s_1, x'_{0,1}, y'_{0,1}$ of camera 1; $\mathbf{U}_{\text{int},2} \in \mathbb{R}^{4\times4}$ is associated with the intrinsic parameters $f_{m,2}, s_2, x'_{0,2}, y'_{0,2}$ of camera 2; $\mathbf{U}_{\text{ext},1} \in \mathbb{R}^{6\times6}$ is associated with the extrinsic parameters $\alpha_1, \beta_1, \gamma_1, {}^{w}\mathbf{P}_{01}^{T}$ of camera 1; $\mathbf{U}_{\text{ext},2} \in \mathbb{R}^{6\times6}$ is associated with the extrinsic parameters $\alpha_2, \beta_2, \gamma_2, {}^{w}\mathbf{P}_{02}^{T}$ of camera 2.

The propagation model between input and output quantities described in section 3, although not very simple, exhibits the advantage of being explicit. Thus, it is possible to compute explicitly the sensitive coefficients as symbolic expressions, and it is not necessary to numerically evaluate them as it often happens with complex applications.

5. COMPATIBILITY ANALYSIS

In not ideal conditions the stereo systems at different positions provides different measurements of the same feature (like the center of mass of a colored spot on surface). Each measurement comes with its uncertainty and a fusion process is suitable to combine them in a unique best estimated one with the associated fused uncertainty. Before fusing points measured from different stereo systems, it is necessary to state if they are associated to the same feature or, statistically speaking, if they belong to the same distribution. Therefore a compatibility analysis of the measured points is performed. A compatibility test on two points $\mathbf{X}_1, \mathbf{X}_2$ with covariances $\mathbf{C}_1, \mathbf{C}_2$ is based on the consideration that the difference $\mathbf{X}_1 - \mathbf{X}_2$ is distributed with zero mean and covariance $\mathbf{C}_1 + \mathbf{C}_2$. On Gaussian assumption, the Mahalanobis Distance (MD) $D^2 = (\mathbf{X}_1 - \mathbf{X}_2)^T (\mathbf{C}_1 + \mathbf{C}_2)^{-1} (\mathbf{X}_1 - \mathbf{X}_2)$ has a χ^2 distribution with a degrees of freedom ν equal to the dimension of vectors $\mathbf{X}$. Chosen a confidence level α' it is stated that the two points are compatible if $D^2 \le \chi^2(\nu, \alpha')$. Let $\mathbf{X}_{i,m}$ be the i-th 3D point measured by the stereo system m with covariance $\mathbf{C}_{i,m}$. The analysis is made up of the following steps: from measured points sets Σ_m and Σ_n of stereo system m and n respectively, for each $\mathbf{X}_{i,m}$, it is associated with the point of Σ_n having the minimum MD to $\mathbf{X}_{i,m}$; if the compatibility test is passed, the association is accepted and the associated couple is fused obtaining the best estimate:

$$\mathbf{X}^*_{k,mn} = \mathbf{C}_{i,n}(\mathbf{C}_{i,m} + \mathbf{C}_{j,n})^{-1}\mathbf{X}_{i,m} + \mathbf{C}_{i,m}(\mathbf{C}_{i,m} + \mathbf{C}_{j,n})^{-1}\mathbf{X}_{j,n}$$

And its covariance matrix:

$$\mathbf{C}^*_{k,mn} = \mathbf{C}_{i,n}(\mathbf{C}_{i,m} + \mathbf{C}_{j,n})^{-1}\mathbf{C}_{i,m}$$

otherwise $\mathbf{X}_{i,m}$ is kept as best estimate of the feature; the process between all the best estimates just obtained is iterated (including the points not associated of the two sets), and a new set Σ_p is obtained. Ambiguous cases can occur, when one point of set Σ_n is compatible with two or more points of set Σ_m. The threshold α' has to be tuned in order to both keep low the ambiguity cases and not to lose useful information.

6. EXPERIMENTAL RESULTS

An inclined can provided with colored markers on its lateral surface and positioned by a Cartesian robot, is acquired by two stereo systems, which are angularly spaced apart of nearly 90°, as illustrated in Fig.1. Starting from an initial position the can is translated along a straight trajectory to a final position and the markers on its surface are acquired both in the initial and final position. In Fig.2 it is possible to see the two acquired positions.

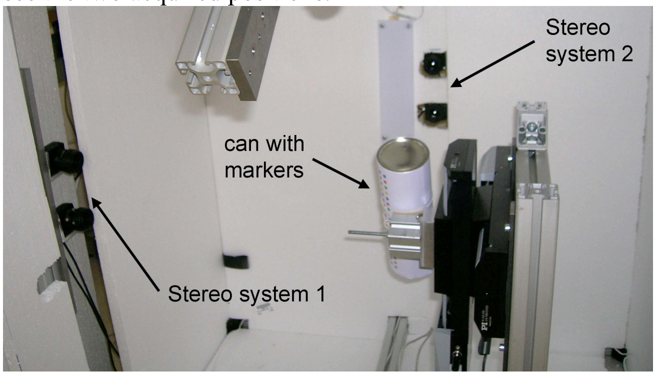

Fig. 1: Picture of the two stereo systems employed for the compatibility analysis.

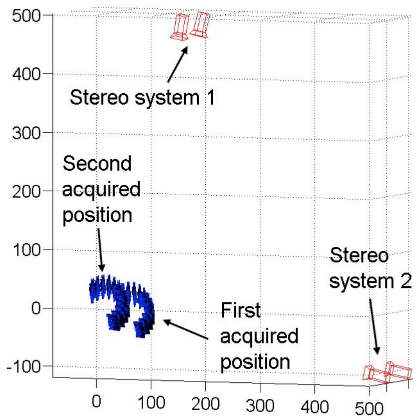

Fig. 2: Sets of points acquired in the two positions.

The acquired colored markers yield two sets of points Σ_1, Σ_2, whose compatibility is analysed as described in section 5. The minimum Mahalanobis distance between each point of Σ_1 and all points of Σ_2 is depicted in Fig.3 for the first position; very similar results are obtained for the second position.

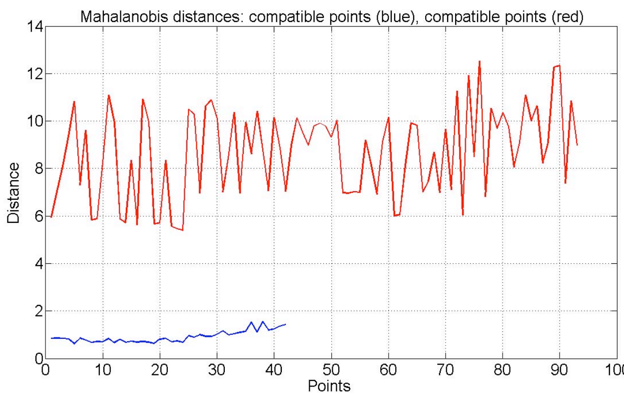

Fig. 3: Minimum Mahalanobis distance between each point acquired by the first stereo system and all points acquired by the second stereo system in the first position of the can.

Fig.3 shows that in the considered case of stereo systems spaced apart of 90°, there is a wide range (about from 1.7 to 5.6) of selectable limit distance (which divides compatible and not compatible points), if the minimum distance between a point of Σ_1 and all points of Σ_2 is considered. In this work, with a selected level of confidence equal to 68.3% and three degrees of freedom, a limit distance equal to 1.88 is obtained. Fig.4 depicts two points belonging respectively to the sets Σ_1, Σ_2, and having a Mahalanobis distance equal to 5.9 which means the two points are considered not compatible. The following two Figs. 5 -6 illustrate two examples of compatibility: a distance of 0.61 which means very good compatibility (Fig.5) and a distance of 1.54 which is associated to a poor compatibility (Fig.6).

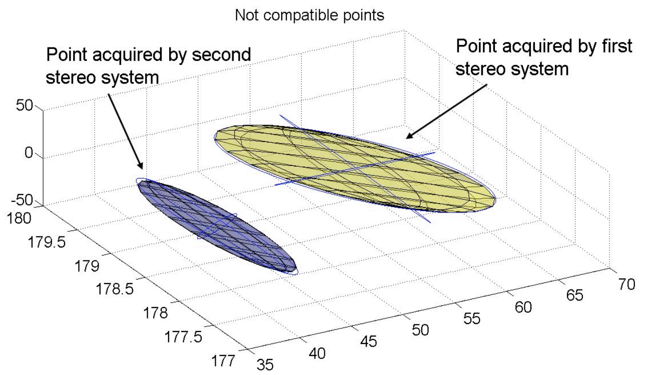

Fig. 4: Example of points acquired by different stereo systems with Mahalanobis distance equal to 5.9 (not compatible).

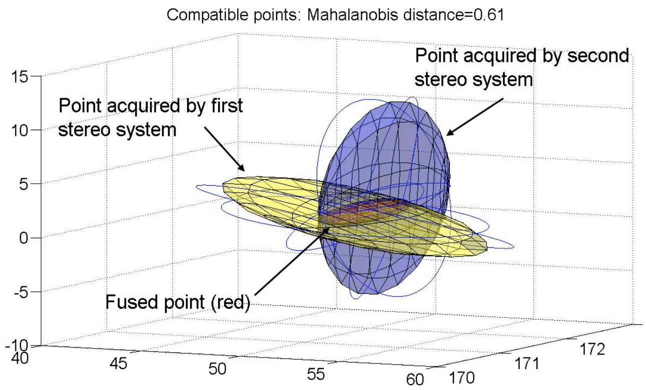

Fig. 5: Example of points acquired by different stereo systems with Mahalanobis distance equal to 0.61 (very good compatibility).

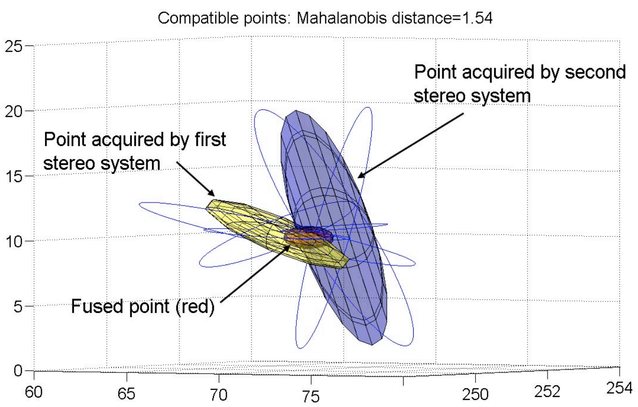

Fig. 6: Example of points acquired by different stereo systems with Mahalanobis distance equal to 1.54 (poor compatibility).

If the Mahalanobis distance between a point of Σ_1 and all points of Σ_2 is analyzed (instead of the minimum distance as performed in Fig.3), there are cases that can lead to an ambiguous situation: the minimum distance (0.81 in Fig.7) is widely less than the limit distance, but the there is also another point in Σ_2 with a distance from the considered point of Σ_1 which may be less or similar to the limit distance (2.53 in Fig.7). As already stated, in this work the selected limit distance is 1.88, which allows to avoid these ambiguous situations.

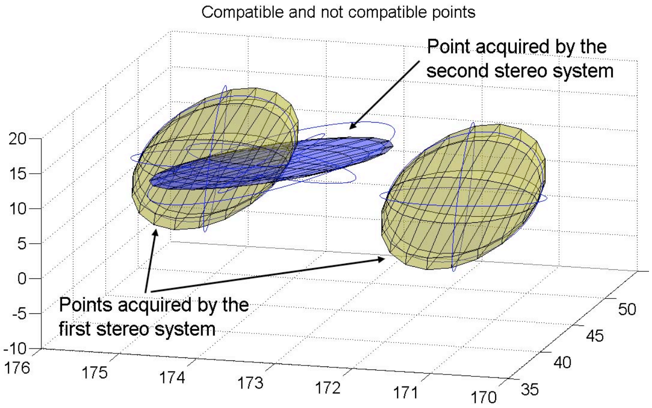

Fig. 7: Example of points acquired by different stereo systems with Mahalanobis distance equal to 0.81 (compatible) and 2.53 (not compatible).

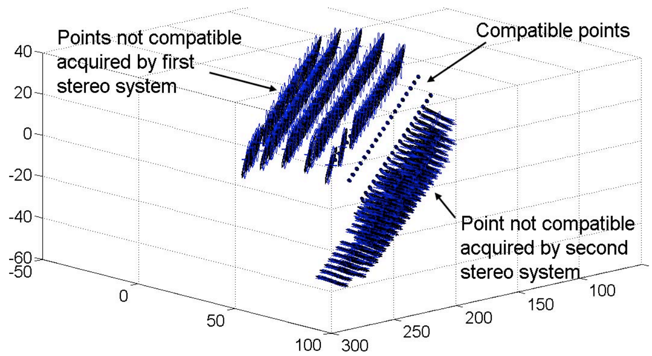

Fig. 8: Picture of the two stereo systems employed for the compatibility analysis.

For the initial position of the can, Fig.8 shows the Σ_p set, comprising the fused compatible points and also the points of Σ_1 and Σ_2 that are not compatible. From Fig.5, Fig.6, Fig.8, it is clear that the uncertainty associated with the fused points is significantly reduced with reference to the uncertainties obtained from a single stereo system. This useful result is particularly true for the two considered stereo systems, since they are angularly spaced apart of 90°.

CONCLUSIONS

This work presented a method for the reconstruction of a 3D shape with superimposed colored markers by means of multiple stereo systems. A detailed uncertainty analysis of the whole method and a statistical compatibility analysis of 3D points acquired by different stereo pairs were included. The described method allows to statistically merge the measurements of different stereo pairs in order to obtain a measurement of a 3D shape and an evaluation of the associated uncertainty. The results showed that positioning the two stereo systems spaced apart of 90° allows to considerably reduce the uncertainty associated to the fused points. The selection of a limit distance, that divides compatible points from not compatible ones, was described.

REFERENCES

[1] M. Celenk, R. A. Bachnak, "Multiple stereo vision system for 3-d object reconstruction", *IEEE Int. Conf. on Systems Engineering*, pp.555-558, Aug 1990.

[2] C. H. Esteban, F. Schmitt, "Multi-Stereo 3D Object Reconstruction", *Computer Vision Image Understanding*, vol. 96, n°.3 Spec.Iss., pp. 367-392, Dec. 2004.

[3] S. Nedevschi, R. Danescu, D. Frentiu, T. Marita, F. Oniga, C. Pocol, "Spatial Grouping of 3D Points from Multiple Stereovision Sensors", *IEEE Int. Conf. Netw. Sens. Control*, vol. 2, pp. 874-879, Mar. 2004.

[4] J. Chen, Z. Ding, F. Yuan, "Theoretical uncertainty evaluation of stereo reconstruction", *II Int. Conf. on Bioinformatics and Biomedical Engineering, ICBBE*, pp. 2378-2381, May 2008.

[5] J. Amat, M. Frigola, A. Casals, "Selection of the best stereo pair in a multi-camera configuration", *IEEE Int. Conf. on Robotics & Automation*, pp.3342-3346,Washington DC, May 2002.

[6] BIPM, IEC, IFCC, ISO, IUPAC, IUPAP, OIML, *Guide to the Expression of Uncertainty in Measurement*, Geneva, Switzerland: International Organization for Standardization, ISBN 92-67-10188-9, 1995

[7] BIPM, IEC, IFCC, ILAC, ISO, IUPAC, IUPAP, OIML, *Evaluation of measurement data—Supplement 1 to the Guide to the Expression of Uncertainty in Measurement—Propagation of distributions using a Monte Carlo method*.

[8] Y. Ma, S. Soatto, J. Kosecka, S. S: Sastry, *An invitation to 3-D Vision*, Springer, 2004.

[9] Berthold K.P. Horn, "Tsai's camera calibration method revisited", http://people.csail.mit.edu/bkph/articles/Tsai_Revisited.pdf, 2000.

[10] Devernay, F., Faugeras, O., "Straight lines have to be straight", *Machine Vision and Applications*, vol. 13, n°. 1, pp. 14-24, August 2001.